Sensor and Simulation Notes

Note 386

23 November 1995

# Radiated Spectra of Impulse Radiating Antennas (IRAs)

D. V. Giri

Pro-Tech, 3708 Mt. Diablo Blvd, Suite 215 Lafayette, CA 94549-3610

## Abstract

Paraboloidal reflector antennas, illuminated by spherical TEM waves, have now been established to possess wide-band and non-dispersive properties. Past analyses have focussed on time-domain characteristics such as the prepulse, the impulse and the postpulse. The postpulse consists of the diffracted fields from the launcher plates and the circular (or of other shape) rim of the paraboloid. These two diffraction terms are small and of opposite signs. Even ignoring the postpulse, the radiated waveform is known to have a net zero area (or no dc component). In this note, the prepulse and impulse part of the radiated waveform has been cast in frequency domain to demonstrate the remarkable bandwidth of such IRAs.

## Acknowledgment

The author wishes to thank Dr. Carl E. Baum of Phillips Laboratory for valuable discussions. He is also thankful to Dr.Donald McLemore of Kaman Sciences Corporation, Dikewood Division and Mr.Bill Prather, Mr.Bob Ayres, Mr.Tyron Tran and Dr.John Gaudet of Phillips Laboratory for their guidance and support.

CLEARED
FOR PUBLIC RELEASE
PL/PA 12-1995

PL 95-0999

## 1. Introduction

A paraboloidal reflector antenna fed by one or more conical transverse electromagnetic (TEM) line(s) has now been established as an efficient radiator of impulse-like waveforms [1 to 9]. In the past, some attempts were made [4] to determine its radiated spectrum by combinations of numerical methods such as method of moments and geometrical optics. However, it was quickly realized that analysis such an IRA was more easily accomplished in time domain. Results of time-domain analyses may be found in [6 and 9]. To a first order approximation, the radiated, on-axis electric field waveform of an IRA, illuminated by a two-arm conical line, sketched in figure 1 is given by [6],

$$\vec{E}(r,\,t) = \frac{D}{4\pi c f_g}\,\frac{1}{r}\left\{\frac{\partial V}{\partial t}(t-T) - \frac{1}{T}[V(t) - V(t-T)]\right\} \tag{1}$$

This equation is later modified for the case of a paraboloidal reflector illuminated by a four-arm conical line. In the above equation, the quantities are:

$$\begin{aligned}
t &\equiv \text{retarded time} = t' - (r/c)\\
t' &\equiv \text{time at which the voltage source is turned on} = 0\\
V(t') &\equiv \text{voltage waveform fed to the TEM line}\\
D &\equiv \text{diameter of the reflector}\\
T &= 2F/c \equiv \text{duration of the prepulse}\\
F &\equiv \text{focal length of the paraboloidal reflector}\\
c &\equiv \text{speed of light in vacuum } (\simeq \text{air}) \simeq 3 \times 10^8 \text{ m/s}\\
f_g &\equiv \text{geometric factor of the TEM line feed} = Z_{feed}/Z_0\\
Z_{feed} &\equiv \text{TEM characteristic impedance of the feed line}\\
Z_0 &\equiv \text{free space characteristic impedance} \simeq 376.97\,\Omega\\
r &\equiv \text{distance to the observer from the focal point, along the optical axis of the reflector}
\end{aligned} \tag{2}$$

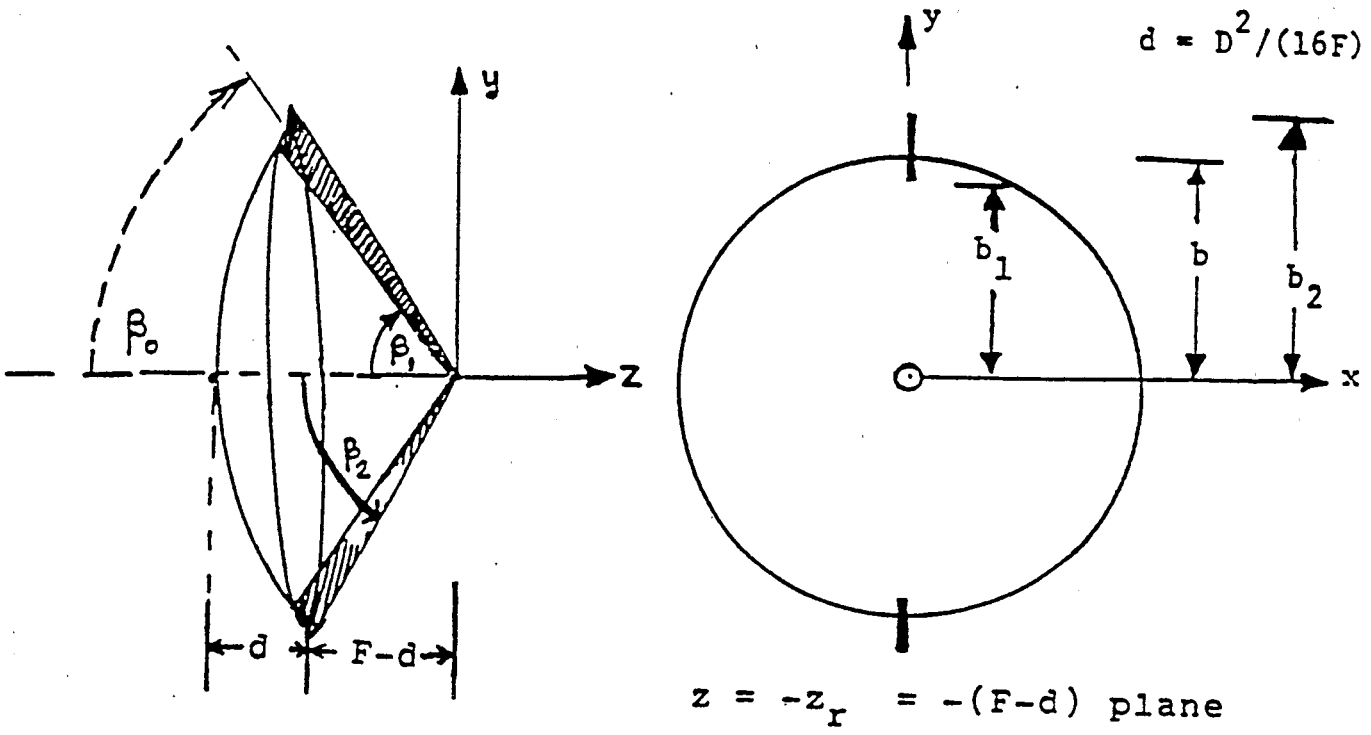


**Figure 1.** The reflector IRA fed by one coplanar-plate conical line

The time-domain radiated field on or off the optical axis has been well known [6 and 9] and also experimentally verified for a prototype IRA [10]. The present interest is in the radiated spectrum of the IRAs. Consider a two-sided Laplace transform of (1) with the complex frequency $s$ denoted by $s = \Omega + j\omega$. Upon setting $\Omega = 0$, one then gets

$$\tilde{\vec{E}}(r, \omega) = \frac{D}{4\pi c f_g} \frac{1}{r} \left\{ e^{-j\omega T} [j\omega \tilde{V}(\omega) - V(0^+)] - \frac{1}{T} [\tilde{V}(\omega) - e^{j\omega T} \tilde{V}(\omega)] \right\} \tag{3}$$

setting the initial condition $V(0^+) = 0$ without any loss of generality and denoting $\omega T = x$, we have

$$\begin{aligned} \tilde{\vec{E}}(r, \omega) &= \frac{D}{4\pi c f_g} \frac{\tilde{V}(\omega)}{r} j\omega \left\{ e^{-jx} - \frac{1}{jx} [1 - e^{-jx}] \right\} \\ &= \frac{D}{4\pi c f_g} j\omega \, e^{-jx/2} \frac{\tilde{V}(\omega)}{r} \left\{ e^{-jx/2} - \frac{\sin(x/2)}{(x/2)} \right\} \\ &= \frac{D}{4\pi c f_g} j\omega e^{-jx/2} \frac{\tilde{V}(\omega)}{r} \left\{ 1 - \frac{2\sin(x)}{x} + \frac{\sin^2(x/2)}{(x/2)^2} \right\}^{1/2} e^{j\phi'(\omega)} \\ &= \tilde{E}_M(r, \omega) \, e^{j\phi(\omega)} \end{aligned} \tag{4}$$

where $\tilde{E}_M$ is the spectral magnitude and $\phi(\omega)$ is the phase function. Denoting the spectrum of the input waveform by,

$$\tilde{V}(\omega) = \tilde{V}_M(\omega) \quad e^{j\phi_v(\omega)} \tag{5}$$

the radiated spectrum can be written as

$$\tilde{E}_M(r, \omega) = \frac{D}{4\pi c f_g} \left\{ 1 - \frac{2\sin(x)}{x} + \frac{\sin^2(x/2)}{(x/2)^2} \right\}^{1/2} \omega \frac{\tilde{V}_M(\omega)}{r} \tag{6}$$

$$\left.\begin{aligned} \phi(\omega) &= \frac{\pi}{2} - \frac{x}{2} + \phi_v(\omega) + \phi'(\omega) \\ \phi'(\omega) &= \arctan\left\{\frac{(x/2)}{\frac{x}{2}\cot\left(\frac{x}{2}\right) - 1}\right\} \\ x &= \omega T = \omega(2F/c) = 2kF = 4\pi(F/\lambda) \\ k &\equiv \text{propagation constant in free space} = \omega/c \end{aligned}\right\} \tag{7}$$

It is noted that, we are yet to specify the input voltage waveform $V(t)$ which leads to $\tilde{V}(\omega)$. In the following setions, we prescribe certain $V(t)$ waveforms and determine the spectral magnitudes of radiated electric fields. Equation (6) is valid whenever $V(t)$ is a regular function and not a distribution. Since practical pulsers generate voltage functions and not distributions (e.g., Dirac delta distribution), this is not a problem in practical situations.

## 2. Step-Function Input Waveform

If $V(t) = V_0\, u(t)$, we have

$$\left.\begin{aligned} \tilde{V}(\omega) &= \tilde{V}_M(\omega)e^{j\phi_v(\omega)} = V_0/(j\omega) \\ \tilde{V}_M(\omega) &\equiv \text{spectral magnitude of the voltage waveform} = V_0/\omega \\ \phi_v(\omega) &\equiv \text{phase function of the voltage wavefore} = -(\pi/2) \end{aligned}\right\} \tag{8}$$

The spectral magnitude of the radiated electric field is obtained by using the above $\tilde{V}_M(\omega)$ into (6) yielding

$$\begin{aligned} \tilde{E}_M^{(s)}(r,\omega) &= \frac{D}{4\pi c f_g}\left\{1 - \frac{2\sin(x)}{x} + \frac{\sin^2(x/2)}{(x/2)^2}\right\}^{1/2}\frac{V_0}{r} \\ &= \left[\frac{D}{4\pi c f_g}\,\frac{V_0}{r}\right]\tilde{f}_s(\omega) \end{aligned} \tag{9}$$

where $f_s(\omega)$ is indicative of the radiated spectrum for a step function input, recalling $x = \omega(2F/c)$. This function $f_s(\omega)$ is shown plotted in figure 2 as a function of the normalized frequency $x$.

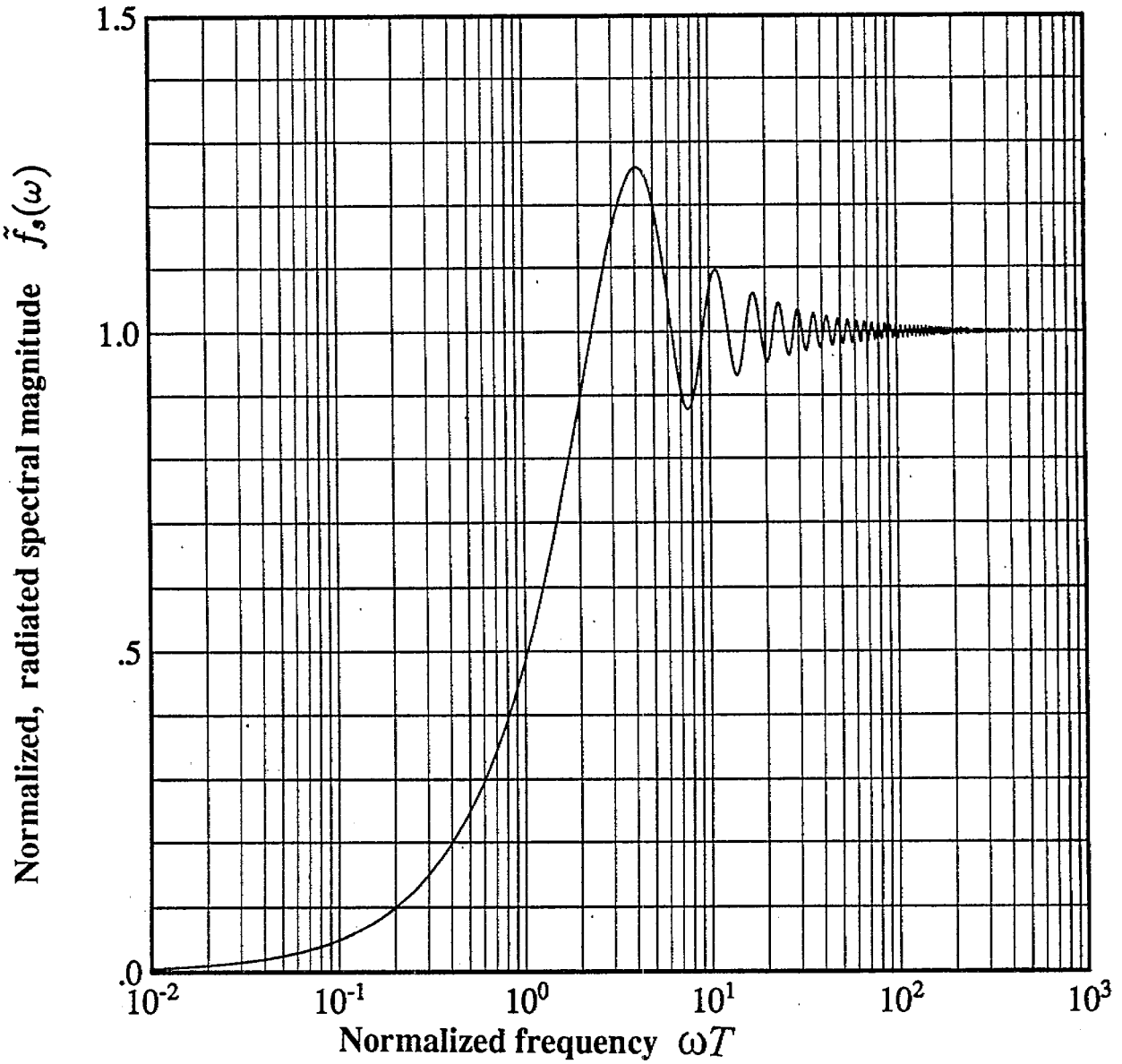


**Figure 2.** Spectral magnitude of the radiated electric field from an IRA for a step-function voltage waveform ($T = 2F/c$ ; $F$ = focal length; $c$ = speed of light in air)

## 3. Double Exponential Input Waveform

We now let the input voltage waveform, as approximated in the case of prototype IRA [10] by,

$$V(t) = V_0(e^{-\beta t} - e^{-\alpha t})u(t) \tag{10}$$

The decay is much slower than the rise ($\alpha \gg \beta$) and the voltage spectrum is given by

$$\tilde{V}(\omega) = \tilde{V}_M(\omega)e^{j\phi_v(\omega)} = V_0\left[\frac{(\alpha-\beta)}{(\beta+j\omega)(\alpha+j\omega)}\right] \tag{11}$$

from which, we have

$$\tilde{V}_M(\omega) = \frac{V_0(\alpha-\beta)}{\sqrt{\beta^2+\omega^2}\sqrt{\alpha^2+\omega^2}} \tag{12}$$

$$\phi_v(\omega) = -[\arctan(\omega/\beta) + \arctan(\omega/\alpha)] \tag{13}$$

The spectral magnitude of the radiated electric field is obtained by using the above $\tilde{V}_M(\omega)$ into (5), yielding

$$\begin{aligned}\tilde{E}_M^{(d.e.)} &= \frac{D}{4\pi c f_g}\left\{1 - \frac{2\sin(x)}{x} + \frac{\sin^2(x/2)}{(x/2)^2}\right\}^{1/2}\frac{V_0}{r}\,\frac{\omega(\alpha-\beta)}{\sqrt{\beta^2+\omega^2}\sqrt{\alpha^2+\omega^2}} \\ &= \left[\frac{D}{4\pi c f_g}\,\frac{V_0}{r}\right]\tilde{f}_{d.e.}(\omega)\end{aligned} \tag{14}$$

where $\tilde{f}_{d.e.}(\omega)$ is the normalized radiated spectrum for a double-exponential voltage input, recalling $x = \omega(2F/c) = \omega T$. It is oberserved that

$$\tilde{f}_{d.e.}(\omega) = \tilde{f}_s(\omega)\frac{\omega(\alpha-\beta)}{\sqrt{\beta^2+\omega^2}\sqrt{\alpha^2+\omega^2}} \tag{15}$$

where $f_s(\omega)$ given in (9), is the radiated spectral magnitude for step function input. This also means,

$$\begin{aligned}\frac{\tilde{E}_M^{(d.e.)}}{\tilde{E}_M^{(s)}} &\equiv \frac{\text{spectral magnitude of the radiated field for double}-\text{exponential input}}{\text{spectral magnitude of the radiated field for step}-\text{function input}} \\ &= \frac{\tilde{f}_{d.e.}(\omega)}{\tilde{f}_s(\omega)} = \frac{\omega(\alpha-\beta)}{\sqrt{\beta^2+\omega^2}\sqrt{\alpha^2+\omega^2}} \equiv \tilde{F}_N(\omega) \\ &= \frac{1-(\beta/\alpha)}{\left[1+\frac{\beta^2}{\alpha^2}+\frac{\omega^2}{\alpha^2}+\frac{\beta^2}{\omega^2}\right]^{1/2}}\end{aligned} \tag{16}$$

Since an unit step function is a limiting case of a double-exponential function with zero risetime and infinite decay time (i.e., $\beta = 0$ and $\alpha = \infty$), the above function $F_N(\omega)$ is seen to approach unity as $\beta \to 0$ and $\alpha \to \infty$, as expected. In the following section dealing with the prototype IRA example, we plot this function $F_N(\omega)$ to estimate the range of frequencies where the prototype IRA performs like an IRA fed with an ideal step function.

## 4. Illustrative Example of the Prototype IRA

A prototype IRA has been fabricated and tested [10 to 14]. It consists of a paraboloidal reflector fed by a pair of 400 $\Omega$ ($f_g \simeq 1.06$) conical transmission lines. One may use the principle of superposition, calculate the radiated fields from one-line feed and then add it vectorially to the fields radiated from the second line feed. The on-axis, radiated electric field for this case is given by

$$\vec{E}(r,t) \simeq \frac{D\sqrt{2}}{4\pi c f_g}\frac{1}{r}\left[\frac{\partial V_p}{\partial t}(t-T) - \frac{1}{T}\{V_p(t) - V_p(t-t)\}\right] \tag{17}$$

$$\tilde{E}_M^{(d.e.)}(r,\omega) \simeq \left[\frac{D\sqrt{2}}{4\pi c f_g}\frac{V_0}{r}\right]\tilde{f}_{d.e.}(\omega) \tag{18}$$

$$V_p(t) = V_0[e^{-\beta t} - e^{-\alpha t}]u(t) \tag{19}$$

$$\tilde{f}_{d.e.}(\omega) = \left[1 - \frac{2\sin(x)}{x} + \frac{\sin^2(x/2)}{(x/2)^2}\right]^{1/2} \frac{\omega(\alpha - \beta)}{\sqrt{\beta^2 + \omega^2}\sqrt{\alpha^2 + \omega^2}} \tag{20}$$

The factor of $\sqrt{2}$ accounts for the vectorial addition of the fields of the due to each conical line. For the prototype IRA described in [10 to 14], the numerical values of the parameters are

$$\begin{aligned}
&D = 3.66 \text{ m} && r = 304 \text{ m} \\
&V_0 = 10^5 \text{ V} && f_g \simeq 1.06 \text{ each line} \\
&c \simeq 3 \times 10^8 \text{ m/s} && F = 1.2 \text{ m} \\
&T = 2F/c \simeq 8 \text{ ns} && x = \omega T = 16\,\pi \times 10^{-9}\, f \\
&\alpha \simeq 2.2 \times 10^{10} \text{ /s} && \Rightarrow \quad t_{10-90} \text{ (rise)} \simeq 100 \text{ ps} \\
&\beta \simeq 5 \times 10^7 \text{ /s} && \Rightarrow \quad t_{e-fold} \text{ (decay)} \simeq 20 \text{ ns}
\end{aligned} \tag{21}$$

In the time domain, substituting the above values gives a peak impulse amplitude of about 4.6 kV/m which is within 10% of the measured value of 4.2 kV/m. Our present interest is in the radiated spectrum which may be calculated by using the numerical values in (18). The results are shown in figure 3. The ultra-wideband nature of the prototype IRA may be seen in this plot. We have also shown in figure 4 the quantity $F_N(\omega)$ which is given by (16) as

$$F_N(\omega) = \frac{1 - (\beta/\alpha)}{\left[1 + \frac{\beta^2}{\alpha^2} + \frac{\omega^2}{\alpha^2} + \frac{\beta^2}{\omega^2}\right]^{1/2}} \tag{22}$$

The plot of $F_N(\omega)$ indicates the range of frequencies over which the prototype IRA with its double-exponential pulser performs like an IRA fed by an ideal step-function source. If we allow a 10% tolerance, this range is seen to be 20 MHz to 2 GHz. More importantly,

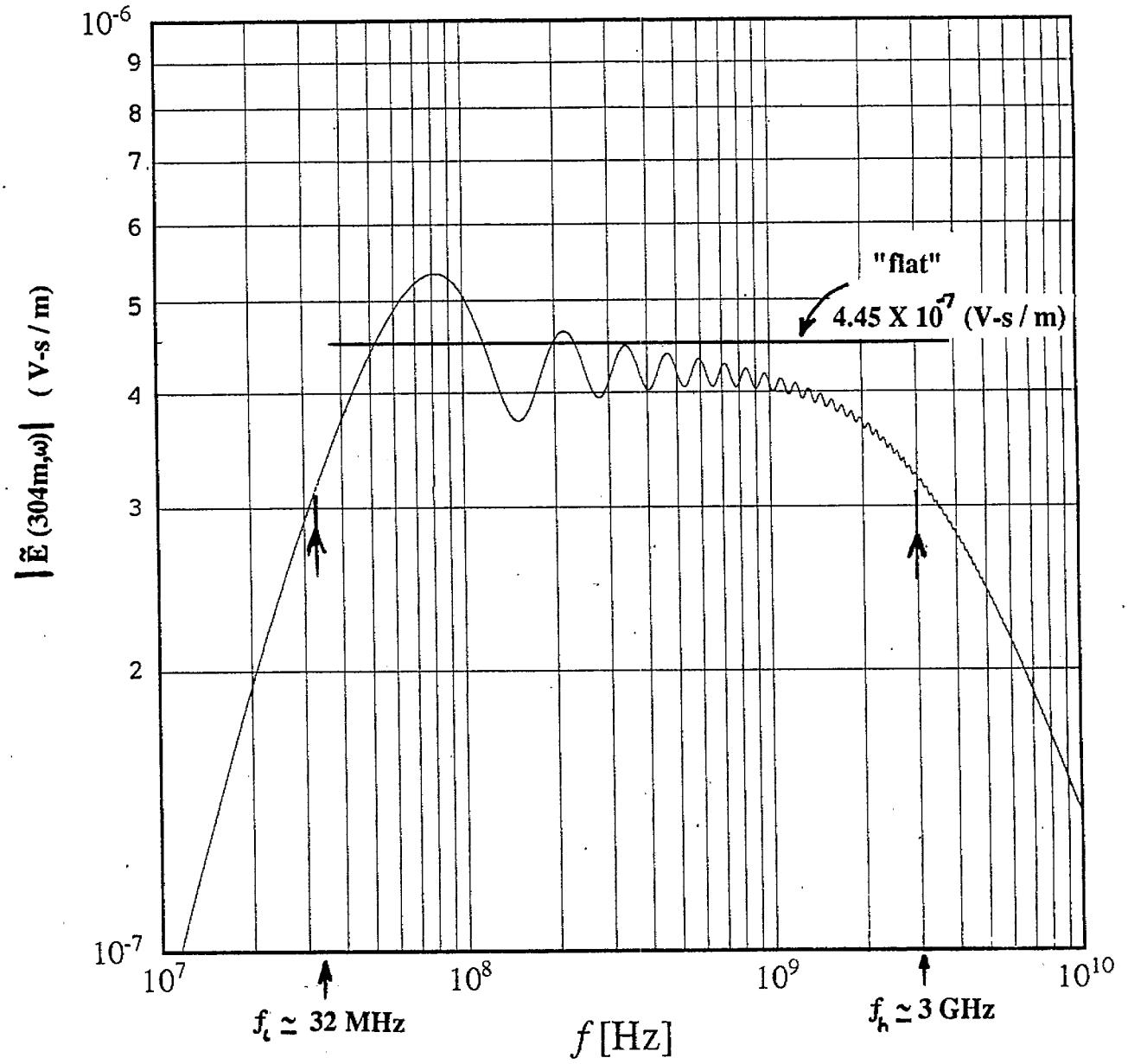


**Figure 3.** Spectral magnitude of the radiated electric field of the prototype IRA at a distance of 304 m along the optical axis

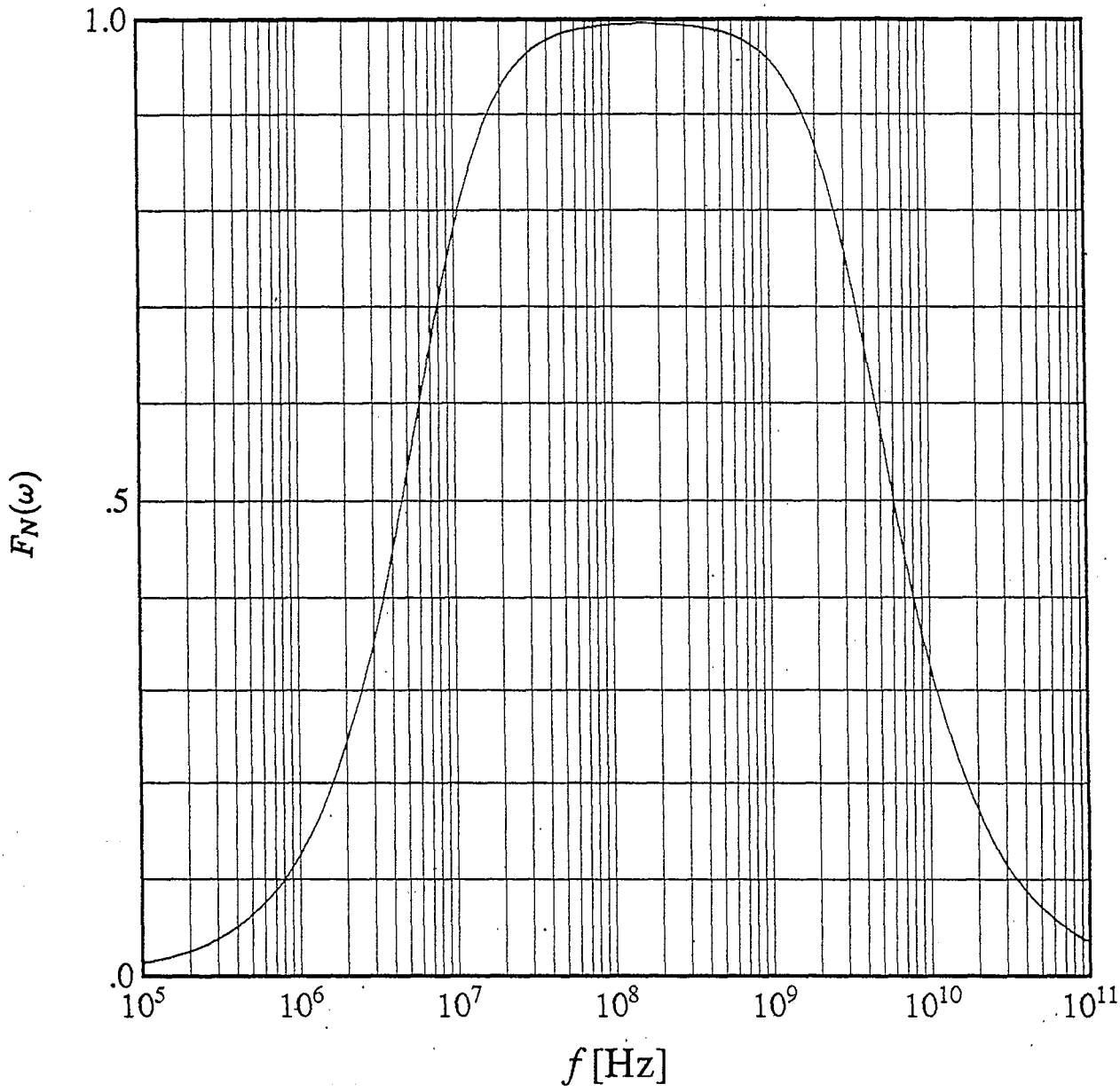


**Figure 4.** Ratio of the spectral magnitude for a double-exponential to a step-function voltage input for the prototype IRA (range independent)

one can estimate the ultra-wide bandwidth of the prototype IRA from its radiated spectral magnitude shown in figure 3. First of all, we have drawn a horizontal line corresponding to a spectral magnitude of $4.45 \times 10^{-7}$ V-s/m. The spectrum is "flat" within $\pm 17\%$ of this value. The low and high frequencies where the spectral magnitude is down by a factor of $(1/\sqrt{2})$ or "3 dB" points are correspondingly $f_\ell \simeq 32$ MHz and $f_h \simeq 3$ GHz leading to the following bandwidth estimates for the prototype IRA.

$$\text{bandratio} \equiv br = (f_h/f_\ell) \simeq 93 \tag{23a}$$

$$\text{relative bandwidth} \equiv rbw = \frac{f_h - f_\ell}{f_h + f_\ell} = \frac{br-1}{br+1} \simeq 0.979 \tag{23b}$$

$$\text{percent bandwidth} \equiv pbw = \frac{f_h - f_\ell}{\left(\frac{f_h+f_\ell}{2}\right)} \times 100 = 200\left(\frac{br-1}{br+1}\right) \simeq 195 \tag{23c}$$

Some observations are in order, concerning this calculated spectrum. We note that the "flat" spectral magnitude of about $4.45 \times 10^{-7}$ V·s/m is in fair agreement [15] with the "measured" spectrum. The measured time-domain boresight electric field at a distance of 304 m was Fourier transformed and the "flat" value was seen to be about $4.68 \times 10^{-7}$ V·s/m [15]. Secondly, the estimated bandratio for the prototype IRA of 93 to 1 is noteworthy, recalling that the antenna is also nondispersive. The percent bandwidth is over 190% out of a theoreitcal maximum of 200%. One of the definitions of "ultrawideband" signal [16] requires a percent bandwidth of over 25%, and the prototype IRA certainly qualifies.

## 5. Summary

To a first-order, the radiated waveforms of a reflector IRA have been known to consist of a prepulse and the impulse of opposite signs and a net zero area. The postpulse consists of diffracted signals from the rim of the reflector and the launcher plates which are in themselves of opposite signs and net zero area. The first-order fields consisting of only the prepulse and impulse have been analytically Fourier transformed in this note for both a step-function input and a fast-rising, slowly decaying voltage waveform modelled by a

double exponential. The spectral magnitudes are plotted in normalized forms and the spectral magnitude for the existing prototype is also displayed. These calculations clearly demonstrate the ultra-wide bandwidth of such antennas in general and of the prototype IRA in particular.

## References


1. C. E. Baum, "Radiation of Impulse-Like Transient Fields," *Sensor and Simulation Note* 321, 25 November 1989.
2. C. E. Baum, "Configurations of TEM Feed for an IRA," *Sensor and Simulation Note* 327, 27 April 1991.
3. C. E. Baum, "Aperture Efficiencies for IRAs," *Sensor and Simulation Note* 328, 24 June 1991.
4. E. G. Farr, "Analysis of the Impulse Radiating Antenna," *Sensor and Simulation Note* 329, 24 July 1991.
5. E. G. Farr and C. E. Baum, "Prepulse Associated with the TEM Feed of an Impulse Radiating Antenna," *Sensor and Simulation Note* 337, March 1992.
6. C. E. Baum and E. G. Farr, "Impulse Radiating Antennas," in *Ultra-Wideband, Short-Pulse Electromagnetics.* edited by H. L. Bertoni et al., pp. 139–147, Plenum Press, NY, 1993.
7. D. V. Giri and S. Y. Chu, "On the Low-Frequency Electric Dipole Moment of Impulse Radiating Antennas (IRAs)," *Sensor and Simulation Note* 346, 5 October 1992.
8. E. G. Farr, C. E. Baum, and C. J. Buchenauer, "Impulse Radiating Antennas Part II," in *Ultra-Wideband, Short-Pulse Electromagnetics 2*, edited by L. Carin and L. B. Felsen, pp. 159–170, Plenum Press, NY, 1995.
9. D. V. Giri and C. E. Baum, "Reflector IRA Design and Boresight Temporal Waveforms," *Sensor and Simulation Note* 365, 2 February 1994.
10. D. V. Giri, H. Lackner, I. D. Smith, D. W. Morton, C. E. Baum, J. R. Marek, D. Scholfield, and W. D. Prather, "A Reflector Antenna for Radiating Impulse-Like Waveforms," *Sensor and Simulation Note* 382, 4 July 1995.
11. D. V. Giri and H. Lackner, "Fabricational Details of Prototype IRAs," *Prototype IRA Memo* 1, 1 May 1994.

12. D. V. Giri and H. Lackner, "Preliminary Evaluation of the Terminating Impedance in the Conical-Line Feed of IRAs," *Prototype IRA Memo* 2, 15 May 1994.
13. D. V. Giri, "Design Considerations of a Uniform Dielectric Lens for Launching a Spherical TEM Wave onto the Prototype IRA," *Prototype IRA Memo* 3, 15 May 1994.
14. D. V. Giri and H. Lackner, "Estimates of Peak Values of Near and Far Fields of Prototype IRAs," *Prototype IRA Memo* 4, 15 May 1994.
15. C. C. Courtney, et al., "Measurement and Characterization of the Impulse Radiating Antenna," *Prototype IRA Memo* 5, 6 September 1995, and private communication in October 1995.
16 *Introduction to Ultra-Wideband Radar Systems*, edited by James D. Taylor, Chapter 1, Section II, p. 2, CRC Press, 1995.